ACTA NEUROBIOLOGIAE EXPERIMENTALIS

Short communication Acta Neurobiol Exp 2011, 71: 381–386

Correlation between formation of the calcarine sulcus and morphological maturation of the lateral ventricle in cynomolgus monkey fetuses

Katsuhiro Fukunishi[1], Kazuhiko Sawada[2,*], Masatoshi Kashima[1], Shigeyoshi Saito[3], Hiromi Sakata-Haga[4], Takayuki Sukamoto[1], Ichio Aoki[3], and Yoshihiro Fukui[4]

[1] Shin Nippon Biomedical Laboratories, Kagoshima, Japan; [2] Laboratory of Anatomy, Dept. of Physical Therapy, Faculty of Medical and Health Sciences, Tsukuba International University, Tsuchiura, Ibaraki, Japan, *Email: k-sawada@tius-hs.jp; [3] MR Molecular Imaging Team, Molecular Imaging Center, National Institute of Radiological Sciences, Chiba, Japan; [4] Department of Anatomy and Developmental Neurobiology, University of Tokushima Graduate School Institute of Health Biosciences, Tokushima, Japan

In the present study developmental changes in the cerebral sulci and volumes of subcortical and archicortical structures of the cerebrum in cynomolgus monkey fetuses were examined with T_1-weighted magnetic resonance (MR) images in 3D. On the embryonic day (ED) 90, the lateral ventricle had still an immature vesicular shape in the occipital region of the cerebrum, and it dramatically closed its lumen by ED 100. In that period the calcarine sulcus progressively infolded from the medial surface of the cerebral hemisphere narrowing the lumen of the lateral ventricle in the occipital region. Volume of the lateral ventricle decreased in the period ED 90–100, increasing afterwards in spite of increasing volumes of subcortical and archicortical structures such as the caudate nucleus, putamen, globus pallidus, amygdala and hippocampal formation. During the same time, the volume of the germinal matrix around lateral ventricles decreased to disappear completely by ED 120. These results suggest that the morphological maturation of lateral ventricle is linked to the development of calcarine sulcus in cynomolgus monkey fetuses. The degree of infolding of calcarine sulcus on ED 100 would be useful as a gross anatomical landmark for evaluating the cerebral maturation in cynomolgus monkey fetuses.

Key words: fetus, macaque, MRI, phylogeny, volume rendering

Cynomolgus monkeys are popular laboratory primates frequently used for Developmental and Reproductive Toxicity testing (called also "teratology testing") when rodents and /or rabbits are not pharmacologically relevant species. In the conventional design of Developmental Toxicity testing using a nonhuman primate, fetuses removed by caesarian section on embryonic day (ED) 100 were used for external, visceral and skeletal examinations (Hendrickx and Cukierski 1987, Chellman et al. 2009). However, a procedure for evaluating the brain abnormality of the monkey fetuses has not yet been established. It is difficult to define brain abnormalities except for definite malformations such as a lissencephaly and exencephalia, because of a complexity of the brain morphology in monkeys.

Some mammalian species including monkeys have a characteristic feature of a convoluted cerebral surface forming sulci and gyri. The primary sulci, i.e., the lateral fissure, calcarine sulcus, central sulcus, parietooccipital sulcus and superior temporal sulcus, are known to be stable within and among primate species (Weiss and Aldridge 2003), and correspond with cytoarchitectural, myeloarchitectural and/or thalamocortical borders (Maudgil et al. 1998). Since the primary sulci emerge in a regular sequence throughout the second half of gesta-

Correspondence should be addressed to K. Sawada
Email: k-sawada@tius-hs.jp

Received 16 December 2010, accepted 7 July 2011

tion in humans (Chi et al. 1977, Garel et al. 2001, Dubois et al. 2008) and monkeys (Fukunishi et al. 2006, Kashima et al. 2008, Sawada et al. 2009), the extent and pattern of the sulcal formations are considered to provide the first clue to cerebral abnormalities, such as a delay in cerebral maturation, agyria, and micropolygyria (Gilles and Gomez 2005). Our previous studies have revealed that the emerging patterns of the primary sulci in cynomolgus monkeys is stable among individuals and comparable with those in humans (Fukunishi et al. 2006, Kashima et al. 2008). Therefore, the development of primary sulci in this primate is considered to be a useful model for investigating the cerebral development and its abnormalities caused by gene defects or by environment insults such as drugs, industrial chemicals and viral infections (Maudgil et al. 1998, Gilles and Gomez 2005).

It is interesting to note that the marked gain in brain weight and demarcation of early-generated cerebral gyri (i.e., parahippocampal gyrus, precentral gyrus, supramarginal gyrus, angular gyrus and cingulate gyrus) are observed in cynomolgus monkey fetuses on ED 100 (the gestation period of this primate is 140–150 days; Fukunishi et al. 2006, Kashima et al. 2008). Thus, EDs 90–100 are considered to be one of the critical periods in the morphological maturations of the cerebrum cortex in cynomolgus monkey fetuses. However, it is still unclear whether a correlation exists between formation of the primary sulci and the development of the subcortical and archicortical structures of the cerebrum on those embryonic days. The aim of this study was to clarify 3D structural changes in the subcortical and archicortical structures of the cerebrum and in the spatiotemporal relation of such structural changes to the development of specific cerebral sulci in cynomolgus monkey fetuses during the period ED 90–100. Recently, using 7-tesla MRI *ex vivo*, we reported highly reproducible gross structural changes in the forebrain (Sawada et al. 2009). Therefore, the present study was conducted using MRI-based volumetric analysis and the 3D configurations of subcortical and archicortical structures in the developing cerebrum of cynomolgus monkey fetuses.

Male and female cynomolgus monkeys (*Macaca fascicularis*) at 3 to 10 years of age were purchased from China National Scientific Instruments nd Materials Import/Export Corporation (Beijing, China) and Guangdong Scientific Instruments and Materials Import/Export Corporation (Gaoyao, China), and maintained in the monkey facility of Shin Nippon Biomedical Laboratories, Ltd. (SNBL; Kagoshima, Japan). Animals were individually housed in stainless-steel cages (68 cm × 70 cm × 77 cm), and kept at 26 ± 3°C and 50 ± 10% relative humidity under 12 h artificial illumination (lights on, 06:00 AM – 06:00 PM). They were given approximately 108 g of pellet diets (Harlan Tekland, Harlan Sprague Dawley Inc., Indianapolis, IN, USA) per day and tap water *ad libitum*. Female monkeys were paired with males on days 12, 13, and 14 of their menstrual cycle. When copulation was confirmed visually, the median day of the mating period (day 13 of the menstrual cycle) was designated as ED 0. Pregnancy was confirmed by ultrasonography (SSD-2000, Aloka Co. Ltd., Tokyo, Japan) on ED 20. Fetuses were removed on EDs 70, 80, 90, 100, 120, 140 and 150, respectively, by caesarian section under inhalation anesthesia of 0.5 – 2.0% isoflurane (Dainippon Pharmaceutical Co., Ltd., Osaka, Japan) in a Na_2O/O_2 (70/30) mixture following an intramuscular injection of a mixture of ketamine hydrochloride (5–10 mg/kg body weight; Sigma, St Louis, MO, USA) and atropine sulfate (0.01 mg/kg body weight; Tanabe Seiyaku Co., Ltd., Osaka, Japan) in 0.9% NaCl. Three male fetuses were used at each embryonic age. The fetuses were deeply anesthetized with an intraperitoneal injection of sodium pentobarbital (25 μg/10 g body weight) and perfused intracardially with 0.9% NaCl followed by 4% paraformaldehyde and 0.2% picric acid in 0.1 M phosphate buffer, pH. 7.4. Brains were removed and immersed in the same fixative. Following the caesarean section, dams were given intramuscular injections of an anodyne, ampicillin sodium (0.4 mg/kg body weight; Meiji Seika Kaisha, Tokyo, Japan) and an antibiotic, buprenorphine hydrochloride (0.02 mg/kg body weight; Otsuka Pharmaceutical Co., Ltd., Tokushima, Japan) once a day for 2 days.

MRI was performed on a 7.0-tesla MRI system (Magnet; Kobelco and Jastec, Japan) (Console; Bruker BioSpin, Karlsruhe, Germany); the frequency is clear from the field. Radiofrequency (RF) coils were selected depending on the size of the samples. A birdcage transmit RF coil (72-mm inner diameter, Bruker BioSpin) and surface receiving RF coil (2-channel phased array, Rapid Biomedical) were used for ED 70–90 samples. A birdcage transmit/receive RF coil (72 mm inner diameter, Bruker BioSpin) was used for ED 100–150 samples. The medial surface of the forebrain was placed on an acryl plate and set horizontally in the buffer. Slice orientations were precisely adjusted using pilot-MR images obtained by gradient-echo sequence: coronal slices were adjusted perpendicular to the medial and ventral surfaces; axial

(horizontal) slices adjusted parallel to the ventral surface were adjusted parallel to the medial surface of the cerebral hemisphere. Then, two-dimensional (2D) T_1-weighted multi-slice spin-echo (SE) anatomical MR images were acquired with the following settings: echo time (TE) = 9.574 ms; repetition time (TR) = 600 ms; slice thickness = 1.25 mm; slice gap = 0 mm; matrix dimension = 256 × 256; RF pulse shape = hermite; slice-ordering = interlaced, and slice orientations = coronal, and axial. The field of view (FOV) was adjusted to the size of the samples and ranged from 2.56 × 2.56 to 6.4 × 6.4 cm. The number of slices selected to cover the entire forebrain by non-gap multi-slice imaging ranged between 10 and 38. The number of averages depended on the selection of receiver coil and the voxel size, and ranged between 4 and 64. Therefore, the total scan time varied between 10 and 163 minutes per 0.5–8.2 hours per sample (10–163 min per image). The gradient-echo pilot-MR imaging was acquired in advance for adjusting the slice orientation of the T_1-weighted MRI with the following parameters: TR = 100 ms, TE = 5 ms, slice thickness = 1.25 mm; matrix dimension = 256 × 256. Slice orientation consisting of coronal was obtained simultaneously using the Tripliot™ method (Bruker BioSpin).

Coronal MR images were used for volumetric analysis. The lateral ventricle, germinal matrix, caudate nucleus, putamen, globus pallidus, lentiform nucleus (putamen plus globus pallidus), amygdala and hippocampal formation were semi-automatically segmented on MR slices using the "Morpho" tool of SliceOmatic software ver 4.3 (TomoVision, Montreal, Canada) based on image contrast as well as user knowledge of the anatomy. The segmented images were then analyzed using the 3D-rendering module of the same software; each cerebral image was rendered in 3D. Those images were then rotated and manipulated in a manner that best visualized the brain morphology. Furthermore, areas of the segmented regions were measured using SliceOmatic software. The volumes were calculated by multiplying the combined areas by the slice thickness (1.25 mm) with the total areas of those regions being regarded as the volume of the whole cerebrum. The criteria for identifying a sulcus using MRI were the same as those in our previous study (Sawada et al. 2009). A clear indentation at the cerebral surface was considered the earliest indication of a sulcus.

This study was approved by the Institutional Animal Care and Use Committee of Shin Nippon Biomedical Laboratories and was conducted in accordance with the Principles of Laboratory Animal Care (No. 86-23, revised 1985 of the National Institutes of Health (NIH)), and with the ethics criteria stated in the bylaws of the Experimental Animal Ethics Committee of Shin Nippon Biomedical Laboratories.

Consistent with our previous study (Sawada et al. 2009), by ED 90 the lateral ventricle still presented an immature vesicular shape in the occipital region, while the other subcortical and archicortical structures such as the caudate nucleus, putamen, globus pallidus, amygdala

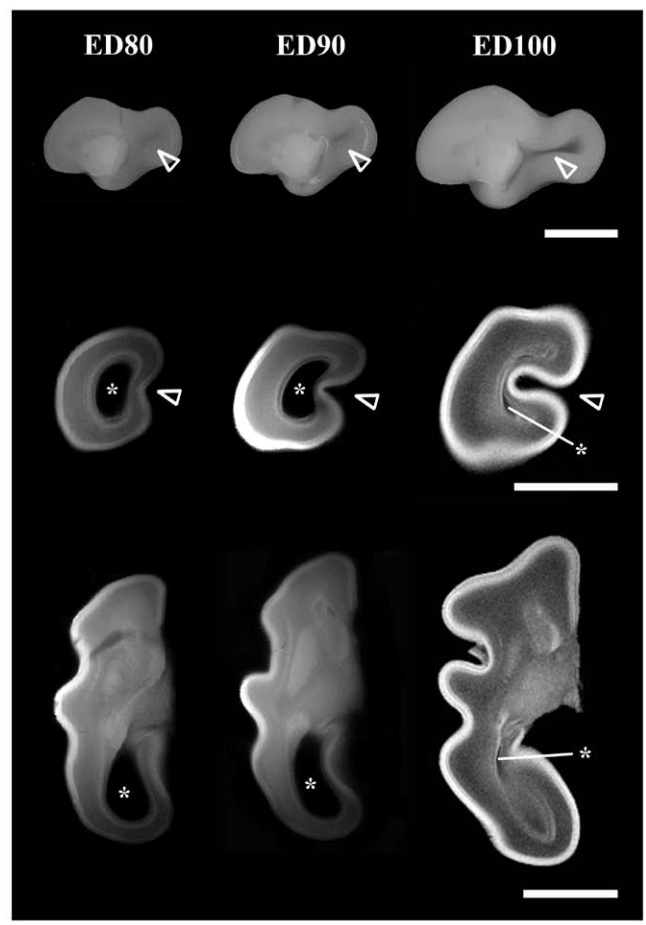

Fig. 1. Changes in calcarine sulcus and vesicular structures of lateral ventricle in occipital region of the cerebrum of cynomolgus monkey fetuses during embryonic days (EDs) 80 to 100 as shown by medial view of cerebral hemisphere (upper row), coronal T_1-weighted MR slices of cerebral hemisphere (middle row) and axial T_1-weighted MR slices of cerebral hemisphere (lower row). Arrowheads indicate indentations of the calcarine sulcus. Asterisks (*) indicate vesicular structures of lateral ventricle in the occipital region. Vesicle had narrowed accompanied by a progressive infolding of the calcarine sulcus on EDs 80–90, and had closed by ED 100. Scale bar is 1 cm..

and hippocampal formation had already developed adult-like features on that embryonic day (Fig. 1). Then lateral ventricles dramatically changed into a more mature shape, closing the vesicular lumen by ED 100. Such changes were clearly observed on axial MR slices (Fig. 1). The calcarine sulcus began to invaginate into the medial cerebral surface on ED 80, and then developed into a definite groove (Fig. 1). The vesicular lumen of the lateral ventricle narrowed in the occipital region of the cerebrum, and then closed in parallel to progression of infolding of this sulcus (Fig. 1).

Volume-rendering images revealed the 3D spatiotemporal morphological changes in subcortical and archicortical structures. During EDs 70–90, the lumen of the lateral ventricle that initially occupied the major part of the volume of cerebral region posterior to the splenium of corpus callosum, gradually disappeared with the progression of infolding of the calcarine sulcus (arrowheads; Fig. 2), and then closed completely by ED 100 (Fig. 2). The germinal matrix of the cerebral hemisphere disappeared in a rostrocaudal gradient between EDs 90 and 120. The germinal matrix surrounding the vesicular lumen of the lateral ventricle was first at the posterior end on ED 100 (Fig. 2). A small mass of germinal matrix was still seen around the rostral horn of the lateral ventricle on ED 120, and it was completely missing on ED 140 (Fig. 2).

During the embryonic days we examined (EDs 70–120), volumes of the subcortical and archicortical structures such as the putamen, globus pallidus, caudate nucleus, amygdala and hippocampal formation increased, while volumes of the lateral ventricle and germinal matrix decreased in parallel (Fig. 3). No left or right side difference was observed in these volumes throughout all the examined period (Fig. 3).

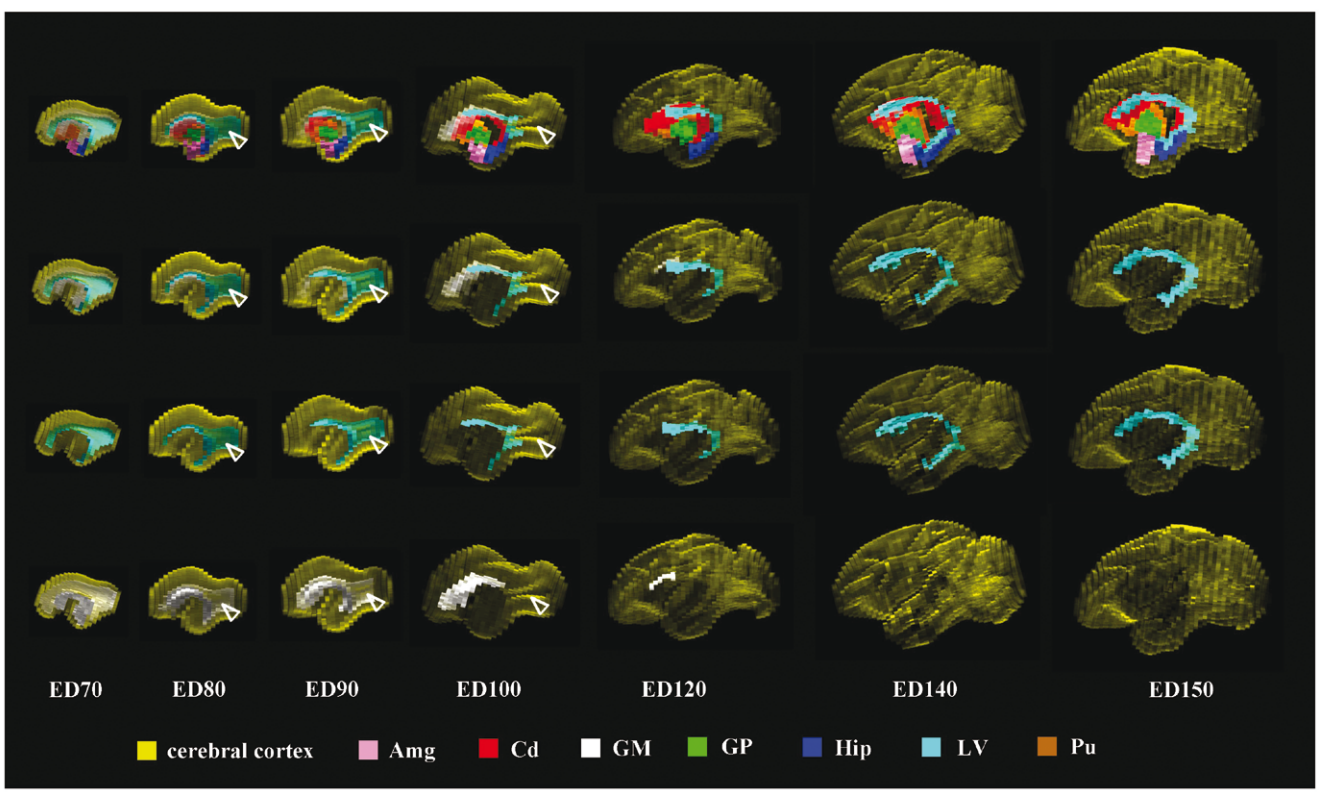

Fig. 2. Volume rendering images of cerebral subcortical structures of cynomolgus monkey fetuses on embryonic days (EDs) 70–100. (Upper row) Reconstructed images of all subcortical structures rendered. (Middle upper row) Reconstructed images of the lateral ventricle (light blue) and germinal matrix (silver). (Middle lower row) Reconstructed images of the lateral ventricle (light blue). (Lower row) Reconstructed images of the germinal matrix (silver). Arrowheads indicate indentations of the calcarine sulcus. Vesicular structures of lateral ventricle disappeared accompanied by progressive infolding of calcarine sulcus during EDs 90–100.
Amg - amygdala (pink), Cd - caudate nucleus (red), GM - germinal matrix (silver), GP - globus pallidus (yellowish green), Hip - hippocampal formation (blue), LV - lateral ventricle (light blue), Pu - putamen (orange).

In the present study, we found that volumes of the lateral ventricle and germinal matrix in the cynomolgus monkey fetuses began to decrease markedly on ED 90, closing the vesicular lumen of the lateral ventricle in the occipital region of the cerebrum by ED 100. The present study further revealed through coronal MR slices and 3D volume-rendering images a correlation between closing of the vesicular lumen and progression of infolding of the calcarine sulcus. Therefore the degree of the calcarine sulcal infolding on ED 100 may be useful for evaluation of the morphological maturation of the lateral ventricle in cynomolgus monkey fetuses.

Our previous study revealed that in the cynomolgus monkey fetuses, adult-like features of subcortical and archicortical structures of the cerebral hemisphere developed by ED 100 (Sawada et al. 2009). However, the volumes of those structures did not reach a plateau throughout all embryonic days examined in the present study, suggesting an increase continuing after birth. Likewise, the entire cerebral volume rapidly increased from ED 100 while still not reaching a plateau by ED 150 (Sawada et al. 2010). On the other hand, in the present study, we found that the lateral ventricle volume reached the minimum by ED 100, and increased again from ED 120. Therefore, the volume of lateral ventricle decreases in relation to morphological maturation of the cerebrum that results in closing of the vesicular lumen of lateral ventricles in the occipital region of the cerebrum by ED 100. Starting from ED 120, the volume of the lateral ventricle increases again, due to further cerebral expansion with higher expansion of the area and volume of the neocortex than those of the subcortical and archicortical structures of the cerebrum.

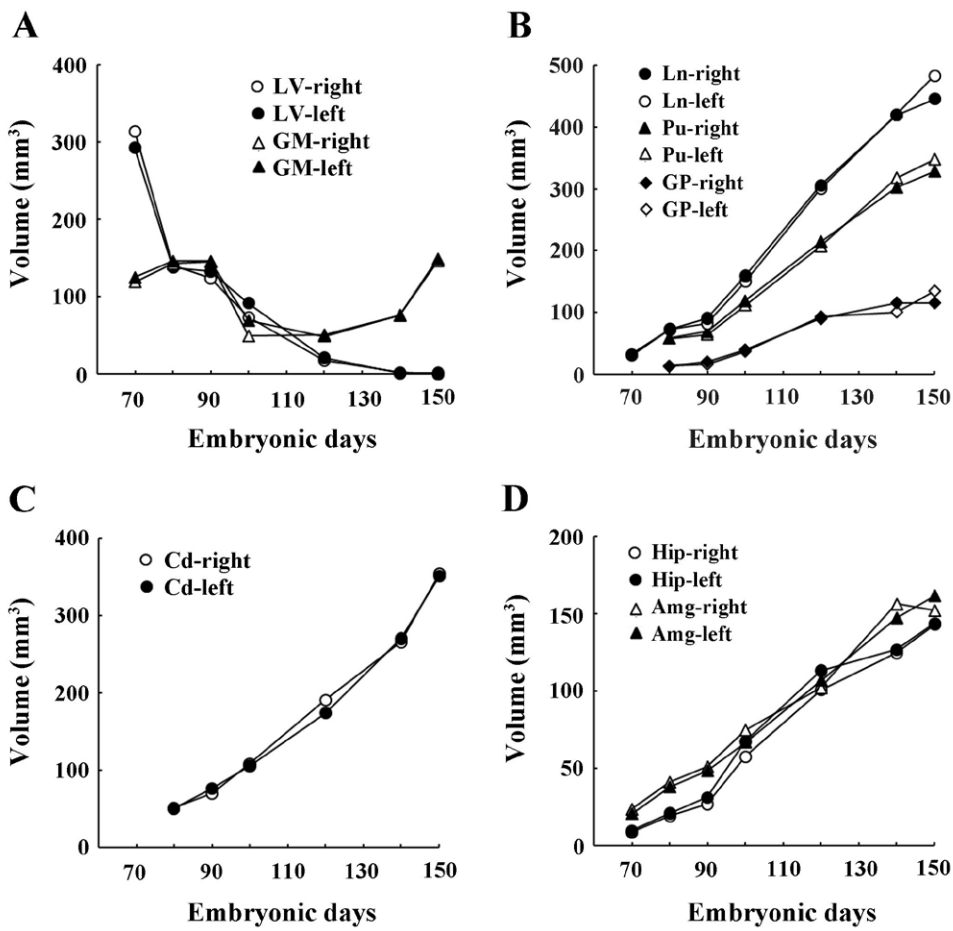

Fig. 3. Developmental changes in volumes of cerebral subcortical and archicortical structures in cynomolgus monkey fetuses from embryonic days (EDs) 70 to 150. (A) Volumes of germinal matrix (GM) 12 and lateral ventricle (LV) of right and left hemispheres. (B) Volumes of lentiform nucleus (Ln), putamen (Pu) and globus pallidus (GP) of right and left hemispheres. (C) Volume of caudate nucleus (Cd) of right and left hemispheres. (D) Volumes of hippocampal formation (Hip) and amygdala (Amg) of right and left hemispheres.

In humans, the volume of the lateral ventricle exponentially increases starting from gestational week (GW) 11, reaching the peak at GW 23, and then diminishing (Kinoshita et al. 2001). Reduction of the volume of the lateral ventricle after GW 23 corresponds with the decrease in volume of the germinal matrix (Kinoshita et al. 2001), in contrast to expansion of the subcortical structures. Thus, the cerebrum of human fetuses experience similar changes in volumes of the lateral ventricle and germinal matrix. The volume of the lateral ventricle begins to decrease following the calcarine sulcus appearing (Chi et al. 1977).

In conclusion, the present study shows that the degree of infolding of calcarine sulcus on ED 100 is useful as a gross anatomical landmark for evaluating maturation of the lateral ventricle in cynomolgus monkey fetuses. Therefore, the present results provide a simple and easy method for evaluating cerebral maturity by gross observations in the conventional design of Developmental Toxicity testing in a nonhuman primate (Hendrickx and Cukierski 1987, Chellman et al. 2009).

This study was supported by Grant-in-Aid for Scientific Research (C) (20590176) from the Japan Society for the Promotion of Science.

Chellman GJ, Bussiere JL, Makori N, Martin PL,Ooshima Y, Weinbauer GF (2009). Developmental and reproductive toxicology studies in nonhuman primates. Birth Defects Res (part B) 86: 446–462.

Chi JG, Dooling EC, Gilles FH (1977) Gyral development of the human brain. Ann Neurol 1: 86–93.

Dubois J, Benders M, Cachia A, Lazeyras F, Leuchter RHV, Sizonenko SV, Borradori-Tolsa C, Mangin JF, Hüppi PS (2008) Mapping the early cortical folding process in the preterm newborn brain. Cereb Cortex 18: 1444–1454.

Fukunishi K, Sawada K, Kashima M., Sakata-Haga H, Fukuzaki K, Fukui Y (2006) Development of cerebral sulci and gyri in fetuses of cynomolgus monkeys (*Macaca fascicularis*). Anat Embryol (Berl) 211: 757–764.

Garel C, Chantrel E, Brisse H, Elmaleh M, Luton D, Oury JF, Sebag G, Hassan M (2001) Fetal cerebral cortex: normal gestational landmarks identified using prenatal MR imaging. Am J Neuroradiol 22: 184–189.

Gilles FH, Gomez IG (2005) Developmental neuropathology of the second half of gestation. Early Hum Dev 81: 245–253.

Hendrickx AG, Cukierski MA (1987) Reproductive and developmental toxicology in nonhuman primates. Prog Clin Biol Res 235: 73–88.

Kashima M, Sawada K, Fukunishi K, Sakata-Haga H, Tokado H, Fukui Y (2008) Development of cerebral sulci and gyri in fetuses of cynomolgus monkeys (*Macaca fascicularis*). II. Gross observation of the medial surface. Brain Struct Funct 212: 513–520.

Kinoshita Y, Okudera T, Tsuru E, Yokota A (2001) Volumetric analysis of the germinal matrix and lateral ventricles performed using MR images of postmortem fetuses. Am J Neuroradiol 22: 382–388.

Maudgil DD, Free SL, Sisodiya SM, Lemieux L, Woermann FG, Fish DR, Shorvon SD (1998) Identifying homologous anatomical landmarks on reconstructed magnetic resonance images of the human cerebral cortical surface. J Anat 193: 559–571.

Sawada K, Sun XZ, Fukunishi K, Kashima M, Sakata-Haga H, Tokado H, Aoki I, Fukui Y (2009) Developments of sulcal pattern and subcortical structures of the forebrain in cynomolgus monkey fetuses: 7-tesla magnetic resonance imaging provides high reproducibility of gross structural changes. Brain Struct Funct 213: 469–480.

Sawada K, Sun XZ, Fukunishi K, Kashima M, Satio S, Sakata-Haga H, Tokado H, Aoki I, Fukui Y (2010) Ontogenetic pattern of gyrification in fetuses of cynomolgus monkeys. Neuroscience 167: 735–740.

Weiss K, Aldridge K (2003) What stamps the wrinkle on the brow. Evol Anthr 12: 205–210.